INS-1 Cells Undergoing Caspase-Dependent Apoptosis Enhance the Regenerative Capacity of Neighboring Cells

Caroline Bonner,[1] Siobhán Bacon,[2] Caoimhín G. Concannon,[1] Syed R. Rizvi,[2] Mathurin Baquié,[3] Angela M. Farrelly,[2] Seán M. Kilbride,[1] Heiko Dussmann,[1] Manus W. Ward,[1] Chantal M. Boulanger,[4] Claes B. Wollheim,[3] Rolf Graf,[5] Maria M. Byrne,[2] and Jochen H.M. Prehn[1]

OBJECTIVE—In diabetes, β-cell mass is not static but in a constant process of cell death and renewal. Inactivating mutations in transcription factor 1 (*tcf-1*)/hepatocyte nuclear factor1a (*hnf1a*) result in decreased β-cell mass and HNF1A–maturity onset diabetes of the young (HNF1A-MODY). Here, we investigated the effect of a dominant-negative HNF1A mutant (DN-HNF1A) induced apoptosis on the regenerative capacity of INS-1 cells.

RESEARCH DESIGN AND METHODS—DN-HNF1A was expressed in INS-1 cells using a reverse tetracycline-dependent transactivator system. Gene(s)/protein(s) involved in β-cell regeneration were investigated by real-time quantitative RT-PCR, Western blotting, and immunohistochemistry. Pancreatic stone protein/regenerating protein (PSP/reg) serum levels in human subjects were detected by enzyme-linked immunosorbent assay.

RESULTS—We detected a prominent induction of *PSP/reg* at the gene and protein level during DN-HNF1A–induced apoptosis. Elevated PSP/reg levels were also detected in islets of transgenic HNF1A-MODY mice and in the serum of HNF1A-MODY patients. The induction of *PSP/reg* was glucose dependent and mediated by caspase activation during apoptosis. Interestingly, the supernatant from DN-HNF1A–expressing cells, but not DN-HNF1A–expressing cells treated with zVAD.fmk, was sufficient to induce *PSP/reg* gene expression and increase cell proliferation in naïve, untreated INS-1 cells. Further experiments demonstrated that annexin-V–positive microparticles originating from apoptosing INS-1 cells mediated the induction of *PSP/reg*. Treatment with recombinant PSP/reg reversed the phenotype of DN-HNF1A–induced cells by stimulating cell proliferation and increasing *insulin* gene expression.

CONCLUSIONS—Our results suggest that apoptosing INS-1 cells shed microparticles that may stimulate *PSP/reg* induction in neighboring cells, a mechanism that may facilitate the recovery of β-cell mass in HNF1A-MODY. ***Diabetes*** **59:2799–2808, 2010**

From the [1]Department of Physiology and Medical Physics, Royal College of Surgeons in Ireland, Dublin, Ireland; the [2]Mater Misericordiae University Hospital, Dublin, Ireland; the [3]Department of Cell Physiology and Metabolism, University Medical Center, Geneva, Switzerland; the [4]Paris-Cardiovascular Research Centre; Institut National de la Santé et de la Recherche Médicale U970, Hopital Européen Georges Pompidou, Paris, France; and the [5]Department of Visceral and Transplantation Surgery, University Hospital Zurich, Zurich, Switzerland.

Corresponding author: Jochen H.M. Prehn, prehn@rcsi.ie.

Received 6 October 2009 and accepted 20 July 2010. Published ahead of print at http://diabetes.diabetesjournals.org on 3 August 2010. DOI: 10.2337/db09-1478.

C.B. and S.B. contributed equally as first authors. M.M.B. and J.H.M.P. contributed equally as senior authors.

Maturity-onset diabetes of the young (MODY) is a familial form of non–insulin-dependent diabetes characterized by early onset of disease, autosomal dominant inheritance, and insulin secretory defects (1). MODY type 3 results from mutations in the gene encoding transcription factor-1/hepatocyte nuclear factor1a (*tcf-1/hnf1a*) (2), recently denoted as HNF1A-MODY. HNF1A belongs to a network of transcription factors controlling organ-specific gene expression during embryonic development and in adult tissues (3). Previous studies demonstrated that HNF1A is expressed in adult β-cells and regulates genes involved in glucose and lipid homeostasis as well as β-cell–specific genes (4–10).

Transgenic mice carrying a deletion of the *hnf1a* gene have defective glucose-stimulated insulin secretion without insulin resistance in target tissues (3), similar to individuals with HNF1A-MODY (11). Findings from animal and cellular models of HNF1A-MODY suggest a decline in functional β-cell mass as the primary mechanism of this defect (8,12,13). Previous studies from our and other laboratories have shown that gene knockout of HNF1A or expression of dominant-negative mutants of HNF1A (DN-HNF1A) inhibits AKT signaling, decreases cell proliferation, and renders cells susceptible to apoptosis (8,14,15). Evidence is growing that β-cell mass is not static but in a constant process of cell death and renewal (16). However, it remains unclear in these models how increased β-cell apoptosis is linked to a compensatory stimulation of regenerative processes.

The Regenerating *(Reg)* gene family belongs to the calcium-dependent lectin gene superfamily (17). Pancreatic stone protein (PSP) was identified from extracts of calcified pancreatic concrements (18). Regenerating protein (*reg*) was independently identified in a screen of a regenerating islet-derived cDNA library taken from 90% depancreatized rats (19) and was found to be identical to PSP (20). Subsequent studies highlighted the potential role for the *Reg* gene family in pancreatic regeneration (21). We investigated the expression of the *PSP/reg* gene during DN-HNF1A–induced apoptosis and found *PSP/reg* to be prominently upregulated. We also provide biochemical evidence that apoptotic cells shed microparticles that may stimulate *PSP/reg* induction in neighboring cells, thereby linking β-cell apoptosis with β-cell regeneration.

RESEARCH DESIGN AND METHODS

INS-1 cells overexpressing HNF1A in an inducible system. Rat insulinoma INS-1 cells overexpressing wild-type HNF1A (WT-HNF1A) or DN-HNF1A under control of a doxycycline-dependent transcriptional activator have been described previously (4,8). Cells were cultured in RPMI-1640 at 6 mmol/l glucose supplemented with 10% FBS (PAA, Cölbe, Germany), 2 mmol/l

L-glutamine, 1 mmol/l pyruvate, 100 units/ml penicillin, 100 μg/ml streptomycin, 10 mmol/l HEPES (pH 7.4), and 50 μmol/l 2-mercaptoethanol (Sigma, Dublin, Ireland). For experiments investigating glucose dependence of *PSP/reg* induction, expression of DN-HNF1A was induced for 24 h and continued for a further 2 h in medium supplemented with glucose at 3, 6, 12, and 18 mmol/l. For caspase inhibition, cells were preincubated with 100 μmol/l of the broad-spectrum caspase inhibitor zVAD.fmk (Bachem, St. Helen's, U.K.) for 45 min prior to induction.

Real-time quantitative RT-PCR. cDNA synthesis was performed using 1.5 μg total RNA as the template and Superscript II reverse transcriptase (Invitrogen, Paisley, U.K.) primed with 50 pmol random hexamers (New England Biolabs, Ipswich, MA). Real-time PCR was performed using the LightCycler 2.0 (Roche Diagnostics, Indianapolis, IN) and the QuantiTech SYBR Green PCR kit (Qiagen). Specific PCR primers were designed using Primer3 software (sequences available on request). For absolute quantification of *hnf1a* copy number, a gene-specific PCR amplicon of known concentration was prepared as a standard. Melting curve analysis and gel electrophoresis was utilized to verify specificity of all PCR products. The data were analyzed using LightCycler software, version 4.0, with all samples normalized to β-actin.

Western blotting. For Western blotting analysis, 25 μg protein lysates were obtained from INS-1 cells overexpressing WT-HNF1A and DN-HNF1A as described (9). The rabbit polyclonal anti-PSP/*reg* antibody (22) was diluted 1:20,000 in Tris-buffered saline containing 1% bovine serum albumin. The primary mouse monoclonal anti–β-actin antibody was utilized at a 1:10,000 dilution (Sigma). Horseradish peroxidase–conjugated secondary antibodies were obtained from Pierce and detected using SuperSignal West Pico Chemiluminescent Substrate (Pierce) and imaged using a FujiFilm LAS-3000 imaging system (Fuji, Sheffield, U.K.).

Immunohistochemistry. Paraffin-embedded pancreatic sections from rat insulin promoter (RIP)-DN-HNF1A and control wild-type C57BL/6JBomTac mice (13) were deparaffinized and incubated overnight at 4°C with the rabbit polyclonal anti-PSP/reg antibody diluted 1:20 (22). Specificity of the antibody was confirmed by Western blotting experiments using recombinant human PSP/reg protein as a control. Slides were incubated for 1 h at room temperature in rhodamine-labeled anti-rabbit secondary antibody (1:100; Jackson Immunoresearch, Suffolk, U.K.). Slides were incubated again overnight at 4°C with the second primary guinea pig anti-insulin antibody (1:20; DakoCytomation A0564) followed by 1 h at room temperature in fluorescein isothiocyanate (FITC)-labeled anti-goat secondary antibody (1:100; Jackson Immunoresearch) and mounted in Vectashield with DAPI (Vector Shield; Vector Labs, Burlingame, CA). Images were taken with a Zeiss LSM710 confocal microscope equipped with a 40 × 1.3NA oil-immersion objective (Carl Zeiss, Jena, Germany). FITC was excited at 488 nm with an argon laser, using a 488/543-nm multichroic beam splitter, and the emission was collected at a 490- to 550-nm spectral band. Rhodamine was excited at 543 nm with a helium neon laser, using the same beam splitter, and the emission was collected at a 570- to 650-nm spectral band. DAPI was excited using the 405 nm DPSS laser and a 405-nm dichroic beam splitter. DAPI fluorescence was detected in the 420- to 480-nm spectral band. Images were processed using Zeiss LSM 4.2 software (Carl Zeiss). Rhodamine-positive cells in the periphery and interior of the islet were quantified as a percentage of total islet cells using Image J software.

Determination of caspase-3–like protease activity. INS-1 cells were seeded at 1×10^5 per ml on a 24-well plate and allowed to settle overnight. Following treatment cells were lysed in 200 μl lysis buffer (10 mmol/l HEPES, pH 7.4; 42 mmol/l KCl; 5 mmol/l MgCl2; 1 mmol/l phenylmethylsulfonyl fluoride; 0.1 mmol/l EDTA; 0.1 mmol/l EGTA; 1 mmol/l dithiothreitol [DTT]; 1 μg/ml pepstatin A; 1 μg/ml leupeptin; 5 μg/ml aprotinin; and 0.5% 3-[{3-cholamidopropyl}dimethylammonio]-1-propane sulfonate [CHAPS]). Fifty microliters of this lysate was then added to 150 μl reaction buffer (25 mmol/l HEPES, 1 mmol/l EDTA, 0.1% CHAPS, 10% sucrose, and 3 mmol/l DTT, pH 7.5) containing 10 μmol/l Ac-DEVD-AMC, which is efficiently cleaved by the apoptotic executioner caspases 3 and 7, among others (23). Cleavage of the substrate DEVD-AMC resulting in the accumulation of fluorescent AMC was measured on a Genios fluorescence plate reader (Tecan) using 355 nm excitation and 460 nm emission wavelengths as previously described (9). Protein content was determined using the Pierce Coomassie Plus Protein assay reagent (Perbio) and activity expressed as change in fluorescent units per microgram of protein per hour.

Detection of nuclear apoptosis. Cells were stained using DAPI to visualize nuclear morphology. Condensed and/or fragmented nuclei were considered apoptotic and observed using an Eclipse TE 300 inverted microscope (Nikon, Dusseldorf, Germany) and a 20 × dry objective, with DAPI excited at 340 ± 25 nm and the emission collected between 450 and 500 nm.

5-Bromo-2-deoxyuridine cell proliferation assay. Cellular proliferation was assessed by means of bromodeoxyuridine (5-bromo-2-deoxyuridine [BrdU]) incorporation using the BrdU Cell Proliferation Assay (Calbiochem). BrdU was added to cells for 24 h, and cells were fixed following treatment. Following incubations with the primary and secondary antibodies, the peroxidase-labeled secondary antibody was detected by addition of substrate solution for 15 min and the reaction stopped. Absorbance was read using a Bio-Rad 550 microplate reader at dual wavelengths of 450/540 nm. The values for the background wells were subtracted from all values. The data were normalized to noninduced control.

TABLE 1
Summary of the study groups used for ELISA measurement of PSP/reg levels

Group	HNF1A-MODY	HNF1A-MODY negative	Type 1 diabetes	*P* value
n	16	7	10	
Sex (female:male)	10:6	4:3	6:4	
Age (years)	35.8 ± 20	27.9 ± 11	31.8 ± 4.9	NS
BMI (kg/m^2)	24.4 ± 4	26.6 ± 7.9	25.5 ± 1.3	NS
A1C (%)	7.6 ± 0.3*	5.4 ± 0.3	7.8 ± 0.3*	$P < 0.05$*
PSP (ng/ml)	18.8 ± 2.7*	8.3 ± 3.8	17.3 ± 1.7*	$P < 0.05$*

Data are means ± SE. Patients were age, sex, and BMI matched. *$P < 0.05$ vs. HNF1A-MODY–negative group.

Microparticle isolation and purification. Cell supernatants were centrifuged (500*g*; 15 min) to remove floating cells and medium containing microparticles released from INS-1 cells collected following an established protocol (24). The medium was filtered using 0.2-μm filters (VWR International, Dublin, Ireland) in order to remove microparticles. Microparticles were analyzed on a Coulter EPICS XL flow cytometer (Beckman Coulter, Villepinte, France) as previously described (25). Regions corresponding to microparticles were identified in forward light scatter and side-angle light scatter dot plots using a logarithmic gain. The gate for microparticles was defined as events with a 0.1- to 1-μm diameter, in comparison with calibrator beads (Megamix fluorescent beads of 0.5, 0.9, and 3 μm in diameter; Biocytex, Marseille, France), and plotted on an FL/FSC dot plot to determine the microparticles. Microparticles were defined as membrane vesicles <1 μmol/l in diameter and expressing externalized phosphatidylserine. Phosphatidylserine was labeled using FITC-conjugated annexin V (Roche Diagnostics, Meylan, France) in the presence or absence (negative control) of CaCl2 (5 mmol/l) as reported earlier (25).

Preparation of recombinant human PSP/reg protein. The recombinant human PSP/reg protein was generated as previously described (22,26). Briefly, the coding region of PSP/reg was cloned into a transfer vector (pPIC9; Invitrogen) containing the signal sequence of the yeast α-mating factor to drive the protein into the secretory pathway.

Subjects and clinical and laboratory measurements. Sixteen diabetic subjects with mutations in the HNF1A gene (P291fsinsC, $n = 9$ and p.Ser353fs, $n = 7$) were identified from an Irish MODY collection. Sequencing of the HNF1A gene was performed by IntegraGen (Bonn, Germany). Control subjects were first-degree relatives of HNF1A-positive subjects who were nondiabetic and negative for the known HNF1A mutation in their pedigree ($n = 7$). In addition, 10 GAD- and/or islet antibody–positive patients with type 1 diabetes were recruited in the Mater Misericordiae University Hospital. Anthropometric measurements including weight, height, and BMI were obtained. The plasma glucose concentration was measured using an YSI analyser (Roche). A1C was determined using high-performance liquid chromatography (Menarini HA81-10, Rome, Italy). Anti-GAD was analyzed using competitive fluid-phase radioimmunoassay by the neuroscience group at John Radcliffe Hospital, Oxford, U.K., and islet cell antibodies by University College London Medical School by similar means. Study groups were matched for age, sex, and BMI as shown in Table 1 and approved by the Mater Misericordiae University Hospital Ethics committee.

PSP/reg enzyme-linked immunosorbent assay. The enzyme-linked immunosorbent assay (ELISA) to quantify human PSP/reg was performed using anti-sera from rabbits and guinea pigs immunized with recombinant human PSP/reg protein as previously described (22,27). Serum was prepared by centrifugation, and the IgG were purified by affinity chromatography on protein A columns. Subsequently, a sandwich ELISA was designed on 96-well ELISA plates. Antibody of the first species (guinea pig) was coated to the bottom, blocked with BSA, and aliquots of serum were then incubated for 2 h. After washing, antibodies of the other species (rabbit) were incubated. Finally, a phosphatase-coupled anti-rabbit IgG was used. Patient serum

PSP/reg levels were compared with standard amounts of protein of recombinant human PSP/reg.

Statistical analysis. Results were expressed as means ± SE. Statistical analysis was conducted using the SPSS version 15.0 software package for Windows (SPSS). Differences between treatments were analyzed by Student *t* test, as well as one-way ANOVA and a subsequent Tukey tests. Nonparametric data were analyzed by Mann-Whitney *U* test. Differences were considered to be significant at $P < 0.05$.

RESULTS

The inducible expression of DN-HNF1A leads to a potent induction of *PSP/reg* mRNA and protein. Inducible, dominant-negative suppression of HNF1A function in INS-1 cells reduces the expression of HNF1A target genes involved in glucose and lipid homeostasis (4) and induces a caspase-dependent apoptosis (8). To investigate the relationship between DN-HNF1A expression, activation of apoptosis, and induction of the regenerative *PSP/reg* gene in particular, INS-1 cells stably transfected with respective rtTA systems were induced to express either DN-HNF1A or WT-HNF1A. We observed a time-dependent induction of DN-HNF1A or WT-HNF1A mRNA in the respective INS-1 cells (Fig. 1*A*). This correlated with a significant reduction in mRNA levels of *pdk1*, a known HNF1A target gene (7), in response to DN-HNF1A expression but not WT-HNF1A (Fig. 1*B*). Examination of the expression of the *Reg* family of genes in INS-1 cells demonstrated that DN-HNF1A led to a potent induction of the *PSP/reg* gene at 24 h (~15-fold) and 48 h (~30-fold). Induction of WT-HNF1A for up to 48 h did not significantly regulate *PSP/reg* expression (Fig. 1*C*).

We next investigated PSP/reg protein levels after induction of DN-HNF1A. Cleavage of PSP/reg converts the 16-kDa proteins into a 14-kDa insoluble fibrillar protein (28). Western blot analysis demonstrated a significant upregulation of the PSP/reg protein (16 kDa) following DN-HNF1A induction and a time-dependent increase in the 14 kDa form of PSP/reg (Fig. 1*D*).

High extracellular glucose levels potentiates *PSP/reg* mRNA induction. We next determined whether the induction of *PSP/reg* mRNA was glucose dependent. Interestingly, we found that the DN-HNF1A induction of *PSP/reg* mRNA expression was modulated by varying extracellular glucose concentrations for 2 h following DN-HNF1A induction. The increase in *PSP/reg* mRNA expression was potentiated in a concentration-dependent manner, with the highest induction evident at 18 mmol/l (Fig. 2*A*).

Elevated PSP/reg levels in an HNF1A-MODY animal model and in the serum of HNF1A-MODY patients. We analyzed paraffin-embedded pancreatic sections from 5-month-old diabetic (Fig. 2*B*) mice expressing DN-HNF1A in β-cells and compared them with wild-type C57BL/6JBomTac mice. Sections were costained for PSP/reg and insulin. PSP/reg was expressed at low levels in wild-type islets (36 ± 1 PSP/reg-positive cells per islet; $n = 8$ islets from $n = 2$ animals) and was found almost exclusively in peripheral islet cells. In contrast, DN-HNF1A islets showed significantly elevated PSP/reg-positive islet cells (82 ± 2 PSP/reg-positive cells per islet; $n = 8$ islets from $n = 2$ animals). Moreover, PSP/reg-positive cells were found to be widespread throughout the transgenic islets and were also detectable in insulin-negative islet cells. Strong expression was also observed in the surrounding acinar cells (Fig. 2*B*). Interestingly, high magnification analysis suggested that many islet cells with elevated PSP/reg immunoreactivity were positioned in the vicinity of cells displaying apoptotic nuclear morphology (Fig. 2*C*).

We next sought to determine whether increased PSP/Reg1a levels could also be detected in HNF1A-MODY diabetic subjects. We analyzed serum PSP/Reg1a levels in a group of 16 diabetic subjects with HNF1A-MODY using ELISA. Results were compared with serum levels in seven HNF1A-MODY–negative, nondiabetic family members. PSP/Reg1a levels were significantly elevated in HNF1A-MODY subjects (Fig. 2*D*). Interestingly, we also detected elevated PSP/Reg1a serum levels in the serum of patients with type 1 diabetes ($n = 10$ patients) (Fig. 2*D*).

Induction of *PSP/reg* mRNA and protein by DN-HNF1A function involves the activation of caspases. Previously we demonstrated that DN-HNF1A–induced apoptosis of INS-1 cells required caspases and involved the activation of the mitochondrial apoptosis pathway (8). To assess whether the activation of executioner caspases influenced DN-HNF1A–induced *PSP/reg* mRNA induction, we first determined the time course of DEVDase activation (indicative of executioner caspase 3/7 activity) by monitoring the cleavage of a fluorigenic caspase substrate. In agreement with our earlier report (8), there was a significant caspase activity in the time frame of 24–48 h post induction. Expression of WT-HNF1A or doxycycline treatment of parental INS-1 cells did not activate caspases (Fig. 3*A*). Furthermore, DN-HNF1A induction mediated nuclear morphological changes indicative of apoptosis with condensation and fragmented nuclei. Pretreatment with the pancaspase inhibitor zVAD.fmk inhibited the occurrence of this apoptotic morphology confirming the caspase dependence (Fig. 3*B*).

Given the similar kinetics of *PSP/reg* mRNA induction and caspase activation, we explored the possibility that caspase activation regulated *PSP/reg* expression. Indeed, DN-HNF1A induction of *PSP/reg* expression was completely inhibited by pretreatment with zVAD.fmk (Fig. 3*C* and *D*). Next we addressed whether DN-HNF1A induction of *PSP/reg* mRNA could be sufficiently explained by its ability to activate apoptosis. Indeed, induction of apoptosis in INS-1 cells with the topoisomerase inhibitor, etoposide, was sufficient to increase *PSP/reg* mRNA levels in a caspase-dependent manner (Fig. 3*E*).

Conditioned medium from DN-HNF1A–induced INS1 cells results in a prominent increase in *PSP/reg* mRNA expression in naïve INS-1 cells. Executioner caspases such as caspase 3 inactivate transcription and translation processes (29), suggesting that apoptosing cells were unlikely to be the source of increased *PSP/reg* mRNA during DN-HNF1A–induced apoptosis. We investigated whether this increased expression was due to apoptosing cells sending a paracrine signal to neighboring cells. After 48 h of DN-HNF1A induction in the presence and absence of zVAD.fmk, the conditioned medium was added directly to naïve INS-1 cells resulting in a 16-fold increase in *PSP/reg* mRNA levels in the naïve INS1-cells (Fig. 4*A*). This induction was absent in cultures incubated with the conditioned medium of zVAD.fmk pretreated DN-HNF1A–induced cells (Fig. 4*A*) or heat-inactivated conditioned medium (Fig. 4*B*), supporting the hypothesis that apoptotic cells secrete heat-sensitive factor(s) that stimulate(s) *PSP/reg* gene induction in neighboring cells.

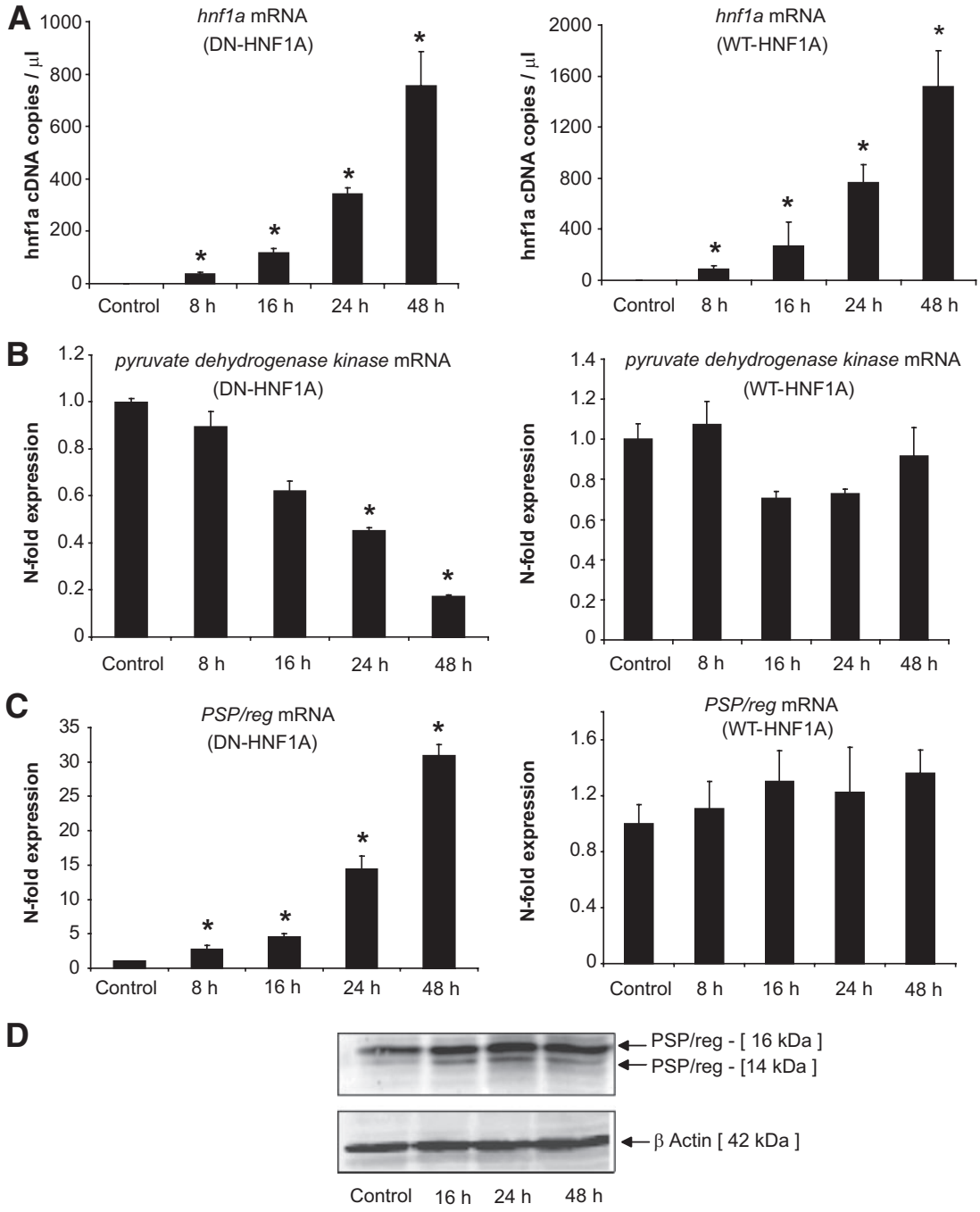

FIG. 1. The inducible expression of DN-HNF1A leads to a potent induction of *PSP/reg* mRNA and protein. *A*: The time course of the *hnf1a* gene induction in DN-HNF1A and WT-HNF1A induced INS-1 cells, represented by absolute quantitative PCR (qPCR). Data are presented as cDNA copy number per microliter. Data are represented as means ± SE from $n = 3$ cultures. The experiment was repeated three times with similar results. *$P < 0.05$ indicates the difference from noninduced controls. *B*: Quantification of the pyruvate dehydrogenase kinase (*Pdk1*) gene expression. DN-HNF1A and WT-HNF1A INS-1 cells were induced with doxycycline from 0 to 48 h. *Pdk1* mRNA expression was examined using real-time qPCR relative to β-actin. Data shown are the means ± SEM of $n = 3$ cultures. The experiment was repeated four times with similar results. *$P < 0.05$, difference from noninduced controls. *C*: Quantification of *PSP/reg* gene expression following DN-HNF1A and WT-HNF1A induction in INS-1 cells. INS-1 cells were treated with 500 ng/ml doxycycline from 0 to 48 h. mRNA expression of *PSP/reg* was examined using real-time qPCR relative to β-actin. Expression levels were normalized to control cells and data represent means ± SEM from $n = 3$ cultures. *$P < 0.05$, difference from noninduced controls. Experiments were repeated six times with similar results (*D*) whole cell lysates (25 μg) were analyzed by Western blotting on 15% SDS-PAGE. Membranes were probed with a polyclonal antibody recognizing PSP/reg. The 14-kDa fragment represents a PSP/reg cleavage product. β-Actin served as a loading control. Approximate molecular weights are provided on the right side of the figure. Similar results were obtained in two separate experiments.

Removal of microparticles inhibits *PSP/reg* gene induction. Microparticles are small (100 nm) membrane vesicles originating from blebbing membranes of apoptotic cells and can be identified by annexin V staining. These microparticles may contain nuclear proteins as well as nucleic acids (30,31). We examined if microparticles were present in our conditioned medium and, if so, whether these could modulate *PSP/reg* expression. After 48 h of DN-HNF1A induction in the presence and absence of zVAD.fmk, we enriched for microparticles in the superna-

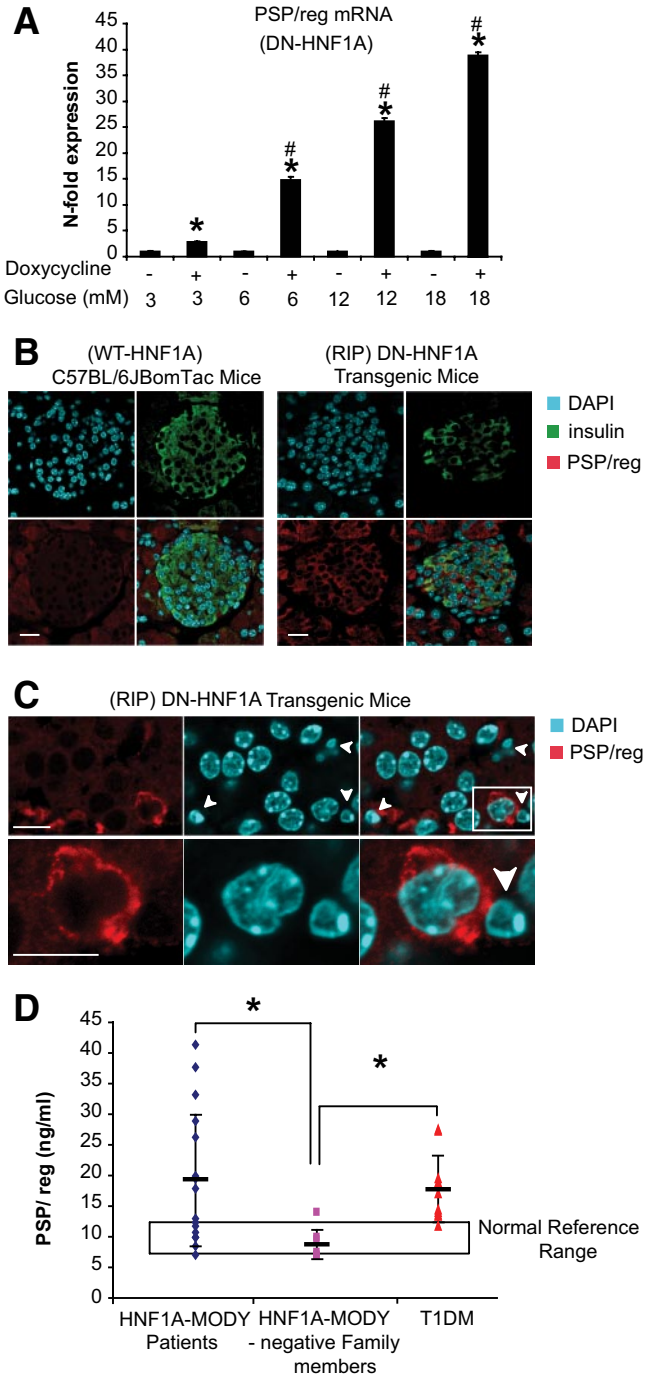

FIG. 2. High extracellular glucose potentiates *PSP/reg* mRNA induction in DN-HNF1A expressing INS-1 cells. *A*: INS-1 cells were induced to express DN-HNF1A for 24 h. Cultures were continued for 2 h at either 3, 6, 12, and 18 mmol/l glucose concentrations. After this period, mRNA expression of *PSP/reg* was analyzed by real-time qPCR. Expression levels were normalized to noninduced control cells and data are represented as means ± SEM from $n = 3$ cultures. *$P < 0.05$, difference from non induced controls; #$P < 0.05$, difference from induced cultures at 3 mmol/l glucose. Experiment was repeated three times with similar results. *B*: PSP/reg immunoreactivity in islet cells in an in vivo mouse model of DN-HNF1A–induced apoptosis. Paraffin-embedded pancreatic sections on slides from 5-month-old wild-type C57BL/6JBomTac control mice and RIP-DN-HNF1A transgenic mice were double stained using antibodies against PSP/reg and insulin. Primary antibodies were recognized by secondary antibodies coupled to Rhodamine (red) for PSP/reg and to FITC (green) for insulin, respectively. Cell nuclei were stained with DAPI (blue). Bar = 10 μm. *C*: PSP/reg immunoreactivity in islets cells in proximity to cells showing apoptotic nuclear morphology. High magnification images of PSP/reg immunoreactivity and DAPI staining in islets of DN-HNF1A mice. Arrows indicate cells exhibiting apoptotic nuclear morphology. Bar = 10 μm. *D*: PSP/reg protein is detectable in the serum of HNF1A-MODY subjects and type 1 diabetic subjects. Serum from HNF1A-MODY patients, their MODY-negative family members, and type 1 diabetic patients were analyzed by a specific ELISA detecting human PSP/reg. The square indicates the normal range (R.G., historic data). Individual values, the average as well as the SD are plotted. PSP/reg levels in HNF1A-MODY and type 1 diabetic subjects were significantly different from MODY-negative, control family members (*$P < 0.05$). (A high-quality digital representation of this figure is available in the online issue.)

tant (25) and applied either filtered or unfiltered medium to naïve INS-1 cells for a further 24 h. Naïve INS-1 cells treated with the unfiltered conditioned medium from DN-HNF1A–induced cells had increased *PSP/reg* mRNA levels that were abolished by filtration of this conditioned medium or by using unfiltered medium from DN-HNF1A–induced cultures in the presence of zVAD.fmk (Fig. 4*C*). Importantly, flow cytometry identified increased microparticle levels in the unfiltered, compared with the filtered, conditioned medium from the same experiment, indicating that microparticles were not generated by the isolation procedure (Fig. 4*D*). Indeed, microparticles were at least 150-fold more abundant in unfiltered compared with filtered conditioned medium with a significantly reduced level in zVAD.fmk pretreated unfiltered medium (Fig. 4*D*). These results suggest that caspases are required for microparticle formation, and their removal abolishes the conditioned medium–induced *PSP/reg* mRNA expression in naïve INS-1 cells.

Treatment of INS-1 cells with recombinant PSP/reg protein reverses the DN-HNF1A–induced decrease in cell proliferation and increases insulin mRNA levels. Animal models of diabetes have demonstrated that recombinant PSP/reg (rPSP/reg) increases β-cell ductal cell proliferation (21,32). DN-HNF1A induction led to significant decreases in cell proliferation as detected by BrdU incorporation, which was reversed by rPSP/reg treatment (Fig. 5*A*). Decreased cell proliferation has been attributed to DN-HNF1A–induced expression of the cell cycle inhibitor $p27^{Kip1}$ (8,9). Induction of DN-HNF1A led to increased $p27^{Kip1}$ mRNA expression but did not affect $p21^{WAF1}$ expression (data not shown), with rPSP/reg cotreatment reducing DN-HNF1A–induced $p27^{Kip1}$ expression (Fig. 5*C*). Furthermore, the rPSP/reg treatment rescued the decrease in *insulin* gene expression induced by DN-HNF1A expression (Fig. 5*B*). Taken together, our data suggest that rPSP/reg treatment reverses the DN-HNF1A–induced phenotype. Indeed, BrdU incorporation was also significantly elevated in naïve INS-1 cells treated with conditioned cultured medium from DN-HNF1A–induced cells compared with those induced in the presence of zVAD.fmk (Fig. 5*D*).

DISCUSSION

The present study provides evidence that β-cell apoptosis may stimulate β-cell regeneration. We demonstrate *1*) that dominant-negative suppression of HNF1A leads to apoptosis and a potent induction of *PSP/reg*; *2*) this induction was potentiated by increased extracellular glucose concentrations; *3*) the induction of PSP/reg was inhibited by the broad-spectrum caspase inhibitor, zVAD.fmk, which also inhibited DN-HNF1A–induced apoptosis; *4*) conditioned medium from DN-HNF1A–induced cells was sufficient to induce *PSP/reg* expression in naïve INS-1 cells, suggesting that apoptosing INS-1 cells secrete factors that stimulate *PSP/reg* induction in neighboring cells; *5*) removal of

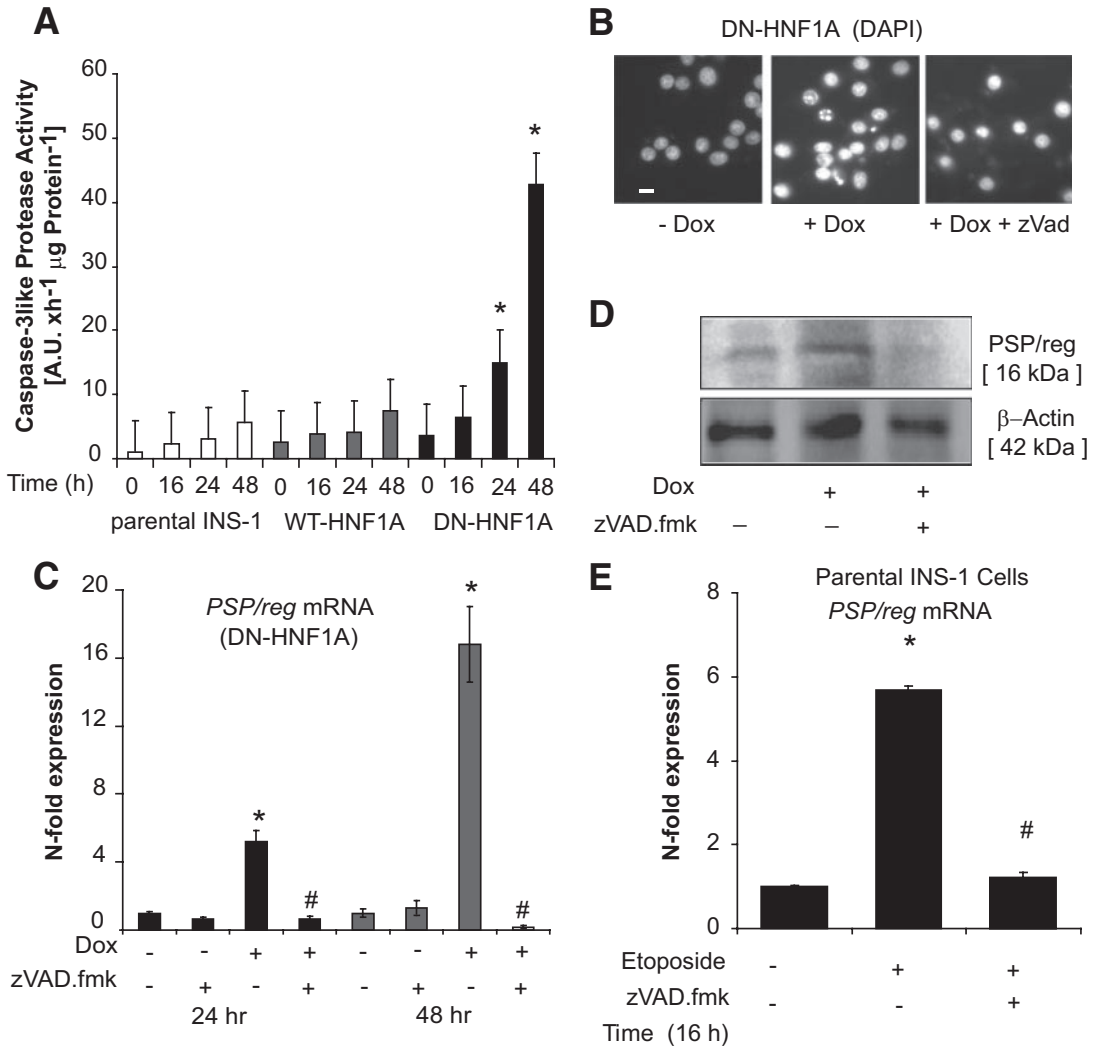

FIG. 3. Activation of caspases during DN-HNF1A–induced apoptosis triggers PSP/reg induction. *A*: Time course of caspase-3–like protease activity in whole-cell extracts. INS-1 cells were induced to overexpress WT-HNF1A or DN-HNF1A for 0, 16, 24, and 48 h. As a control, parental INS-1 cells were treated with doxycycline for 0, 16, 24, and 48 h. Caspase protease activity was measured by cleavage of the fluorigenic substrate Ac-DEVD-AMC (10 μmol/l). Activities are represented as increase in AMC fluorescence (in AU) per 1 h per microgram of protein. Data represent means ± SE from $n = 6$ cultures. Experiments were repeated two times with similar results. *$P < 0.05$, difference from noninduced controls. *B*: Treatment with the broad spectrum caspase inhibitor zVAD.fmk (100 μmol/l) inhibits apoptosis after induction of DN-HNF1A. Cultures were simultaneously pretreated with doxycycline and zVAD.fmk or vehicle (DMSO; zVAD.fmk) for 48. Apoptotic cell morphology was assessed by DAPI staining of nuclear chromatin. *C*: zVAD.fmk inhibits *PSP/reg* mRNA induction. The mRNA expression of *PSP/reg* was examined using real-time qPCR. Expression levels were normalized to noninduced plus noninduced zVAD.fmk–treated control cells. Data are represented as means ± SE from $n = 3$ cultures. *$P < 0.05$, difference from noninduced controls. #$P < 0.05$, difference compared with doxycycline alone–treated cultures. The experiment was repeated three times with similar results. *D*: PSP/reg protein expression was detected by Western blotting. A duplicate experiment showed similar results. Membrane was stripped and reprobed with anti–β-actin as a loading control. *E*: *PSP/reg* gene induction in parental INS-1 cells treated with etoposide is caspase dependent. INS-1 cells were simultaneously treated with etoposide (20 μmol/l) or vehicle (0.1% DMSO) for 24 h in the presence and absence of zVAD.fmk (100 μmol/l). Following treatment, mRNA expression of *PSP/reg* was examined using real-time qPCR. Expression levels were normalized to control cells. Data are represented as means ± SE from $n = 3$ separate cultures. *$P < 0.05$, difference from non induced controls. #$P < 0.05$, difference compared with etoposide alone–treated cultures. Data shown are the mean of $n = 3$ separate experiments.

microparticles from this conditioned medium inhibited *PSP/reg* induction, suggesting that microparticles released from blebbing membranes mediated this effect; *6*) treatment of INS-1 cells with rPSP/reg protein reversed the DN-HNF1A–induced decrease in cell proliferation and *insulin* mRNA; and *7*) moreover, PSP/reg serum levels were significantly elevated in HNF1A-MODY patients and type 1 diabetes compared with HNF1A-MODY–negative, nondiabetic family members.

Regulation of β-cell mass in HNF1A-MODY. Evidence is growing that functional β-cell mass is decreased in animal models of MODY and in type 2 diabetes, with an increased apoptosis rate largely contributing to this decrease (12,13,33). However, a decrease in β-cell mass does not necessarily implicate that new β-cells are not generated during disease progression. Indeed, β-cell mass is a result of a homeostatic balance between the generation of new β-cells and the rate of their apoptosis (34). As HNF1A-MODY and type 2 diabetes evolve over several years or decades, the destruction or apoptosis rate of β-cells may eventually exceed the rate of β-cell generation during disease progression.

Although β-cell regeneration may occur during disease progression, it is not clear whether this happens through self-replication of mature β-cells, through neogenesis of progenitor cells residing in the pancreas or recruited from

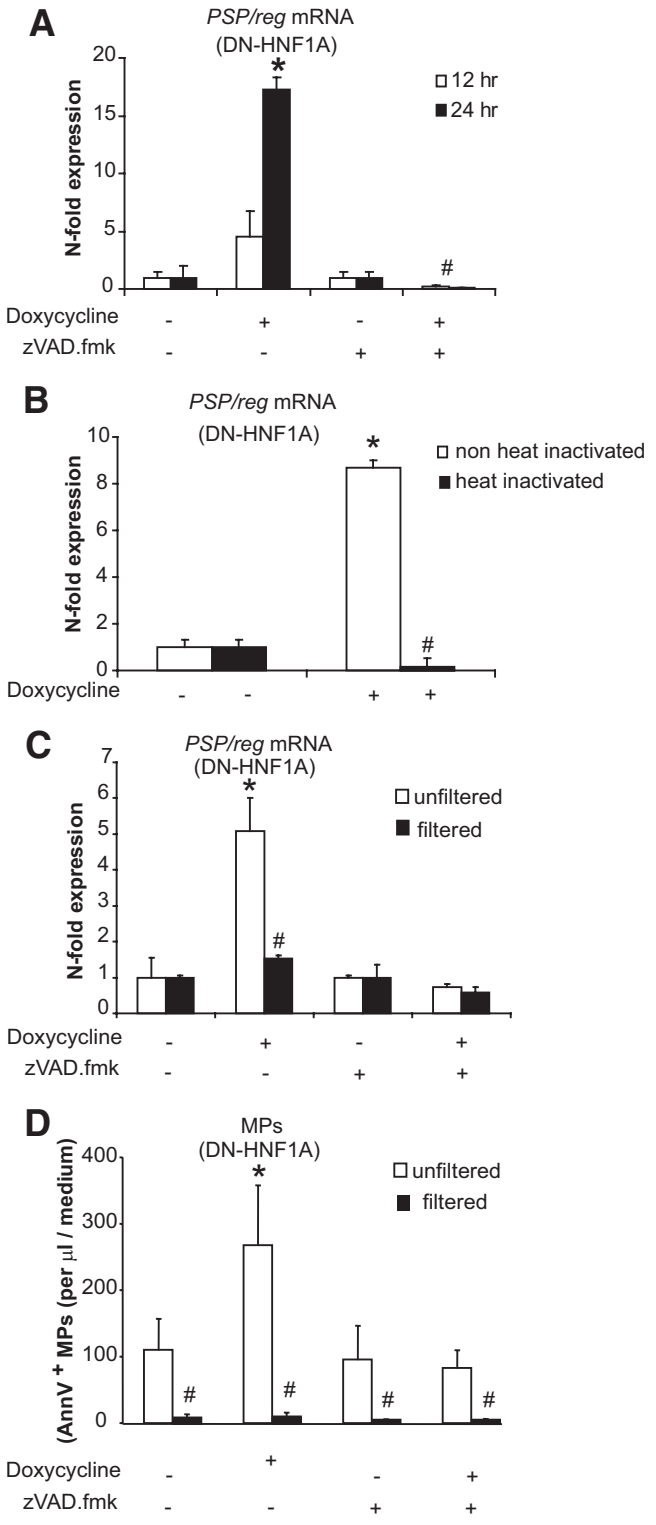

FIG. 4. Conditioned medium from DN-HNF1A–induced INS-1 cells results in a prominent increase in *PSP/reg* mRNA expression in naïve INS1 Cells. *A*: INS-1 cells were induced with 500 ng/ml of doxycycline in the presence and absence of zVAD.fmk (100 μmol/l) at 0.05% serum in 6 mmol/l glucose for 48 h. The conditioned culture medium was added to the noninduced, naive cells for a further 24 h. After treatment, mRNA expression of *PSP/reg* was analyzed by real-time qPCR. Expression levels were normalized to noninduced controls. Data are represented as means ± SE from $n = 3$ cultures. *$P < 0.05$, difference from noninduced controls; #$P < 0.05$, difference from doxycycline alone–treated cultures. Experiments were repeated six times with similar results. *B*: Duplicate experiments of INS-1 cells were induced for 48 h. Conditioned culture medium was heat inactivated at 95°C for 15 min and added to the naive cells for a further 24 h. *PSP/reg* gene expression was analyzed by real-time qPCR. Data are represented as means ± SE from $n = 3$ cultures. *$P < 0.05$, difference from noninduced controls. Experiments were repeated four times with similar results. *C*: The conditioned medium from cells treated as described in *A* above was centrifuged and filtered through 0.20 μm filters and added to naïve INS-1 cells for 24 h. Unfiltered conditioned medium served as a control. *PSP/reg* gene expression was analyzed by real-time qPCR. Data are represented as means ± SE from $n = 3$ cultures. *$P < 0.05$, difference from noninduced controls. Experiments were repeated three times with similar results. *D*: INS-1 cells were induced with doxycycline in the presence and absence of zVAD.fmk. The conditioned culture medium was added to naive cells for a further 24 h. Supernatants were collected and detached cells were precipitated at (300*g*), followed by additional 800*g* centrifugation. Microparticles were quantified as described in RESEARCH DESIGN AND METHODS.

other tissues, or through transdifferentiation. Here, we supply to our knowledge for the first time evidence that the interaction of β-cell apoptosis and regeneration is more complex and in fact that both processes may be mechanistically linked. In our study, we observed that dominant-negative suppression of HNF1A or apoptosis induced by genotoxic stress (etoposide) led to caspase-dependent apoptosis of INS-1 cells, associated with the induction of the regenerative *PSP/reg* gene. Furthermore, conditioned medium from apoptosing cells was sufficient to stimulate *PSP/reg* mRNA expression and BrdU incorporation in naïve INS-1 cells. These findings allow for the conclusion that apoptosing β-cells secrete factor(s) that can stimulate regenerative gene induction and cellular proliferation in neighboring cells. Finally, we demonstrate that administration of rPSP/reg reversed the DN-HNF1A–induced decrease in cell proliferation, supporting the concept that β-cell replication may be positively regulated by β-cell apoptosis. The ability of apoptotic cells to provide signaling cues for their environment has been demonstrated in other settings, such as inhibition of inflammation. Interestingly, recent studies (35,36) have demonstrated that caspase activation is required for tissue regeneration during wound healing and planarian regeneration, suggesting that tissue regeneration in response to caspase-dependent apoptosis may be an evolutionary conserved process.

PSP/reg: biological effects and role in HNF1A-MODY. The Reg family of proteins constitute a multigene family in humans and rodents (19). PSP/reg increases β-cell mass and stimulates β-cell proliferation under physiological conditions and in 90% depancreatized and nicotinamide-injected rats (19,37). Studies in mice lacking the gene *Reg1*, the mouse homologue of *PSP/reg*, revealed that *Reg1* is involved in cell-cycle progression and normal islet growth (37). *Reg1* knockout mice have significant reductions in islet cell mass and rate of DNA synthesis in isolated islet cells (37,38). We identified that rPSP/reg reversed the DN-HNF1A–induced upregulation of $p27^{Kip1}$ gene expression and the concomitant decrease in *insulin* expression. Previous studies have shown that PSP/reg induces extracellular signal–related kinase 1/2 signaling in MKN45 gastric cancer cells (39). However, the signal transduction pathways activated by PSP/reg in pancreatic islets warrant further investigation. Interestingly, we observed that elevated extracellular glucose concentrations rapidly potentiated *PSP/reg* gene expression. This may represent an important physiological feedback loop for the regulation of β-cell mass.

PSP/reg is physiologically secreted from pancreatic acinar cells (20). In the adult rat, PSP/reg has been shown to be present only in small amounts in β-cells (20,40). We

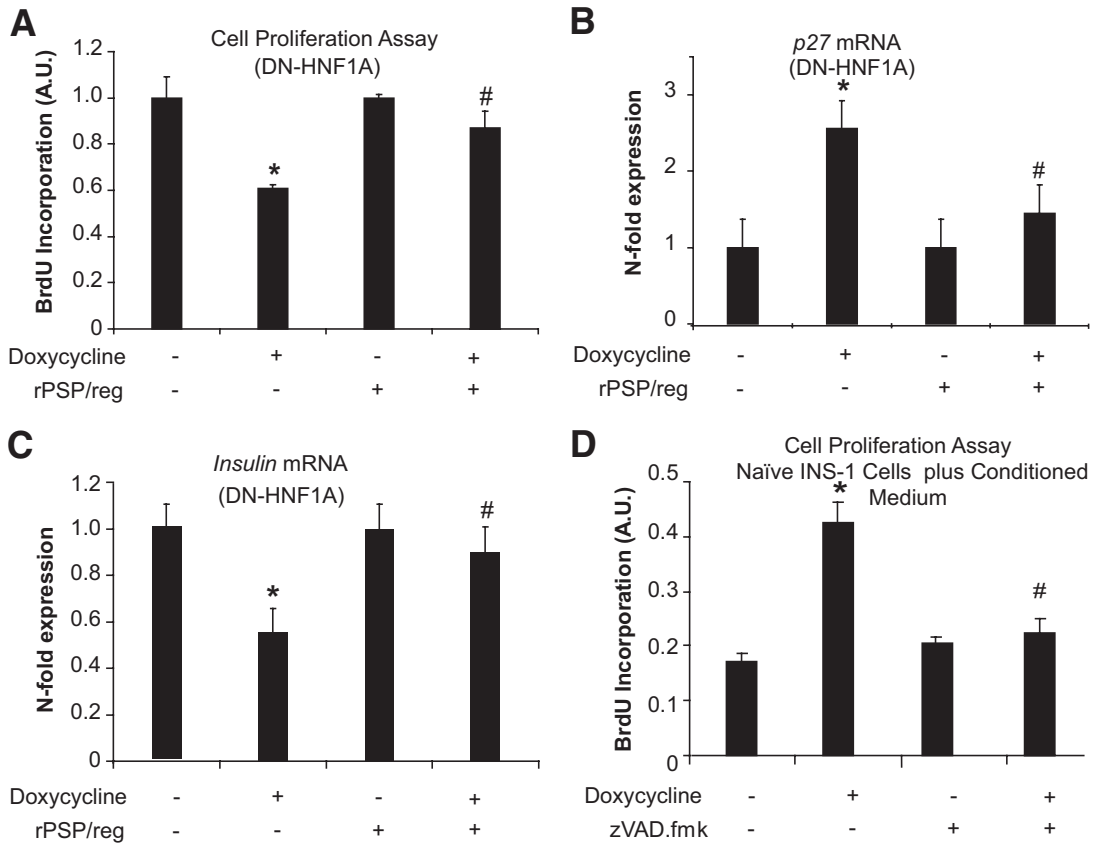

FIG. 5. Treatment of INS-1 cells with recombinant PSP/reg protein reverses the phenotype of HNF1A-MODY cells. *A*: INS-1 cells were induced to express DN-HNF1A for 24 h before being cultured for a further 24 h in the presence and absence of 10 ng/ml of rPSP/reg for 24 h. Proliferation was assessed by BrdU incorporation into the cells. Data are a means ± SE from $n = 6$ cultures. Experiments were repeated three times with similar results. *$P < 0.05$, difference from noninduced controls. #$P < 0.05$, difference compared with doxycycline alone–treated cultures. *B* and *C*: DN-HNF1A INS-1 cells were treated as described in *A* above. *Insulin* (*B*) and $p27^{Kip1}$ (*C*) gene expression was analyzed by real-time qPCR. Data are represented as means ± SE from $n = 3$ cultures. *$P < 0.05$, difference from noninduced controls. #$P < 0.05$, difference compared with doxycycline alone–treated cultures. Experiments were repeated three times with similar results. *D*: The supernatant of apoptosing INS-1 cells induced by DN-HNF1A overexpression is sufficient to stimulate cell proliferation in naïve INS-1 cells. Cells were induced with 500 ng/ml of doxycycline in the presence and absence of zVAD.fmk (100 μmol/l) in 0.05% serum at 6 mmol/l glucose for 48 h. The conditioned culture medium was added to the noninduced, naive cells for a further 24 h. After treatment, cell proliferation was assessed by BrdU incorporation. Data are a means ± SE from $n = 6$ cultures. Experiments were repeated three times with similar results.*$P < 0.05$, difference from noninduced controls. #$P < 0.05$, difference compared with doxycycline alone–treated cultures.

detected increased expression of PSP/reg in insulin-positive islet cells in 5-month-old transgenic HNF1A-MODY mice, confirming previous findings that PSP/reg is expressed in islets during injury and regeneration processes (17,19). Moreover, PSP/reg was also found in insulin-negative islet cells (Fig. 2*B*). In this context, a recent study has suggested α-cells to be the major source of β-cell regeneration/conversion in mice in vivo (41). We also detected increased PSP/reg levels in the serum of HNF1A-MODY patients. We can only speculate whether the source of PSP/reg in the serum of HNF1A-MODY patients was the endocrine or exocrine pancreas (i.e., islet or acinar cells). We can likewise not exclude that these levels came from other organs potentially affected in HNF1A-MODY, such as the liver, where PSP/reg is also expressed (42). However, we also detected elevated levels of PSP/reg in subjects with type 1 diabetes, arguing for a role for pancreatic injury and β-cell apoptosis as a source for elevated PSP/reg serum levels.

Microparticles as signal transducers or enablers. In our study, we detected that apoptotic INS-1 cells released annexin V–positive microparticles into the medium in a caspase-dependent manner. Microparticles are being increasingly described as efficient vehicles for the release of signaling molecules. Microparticles enable communication between different cell types (43) and also deliver proteins to cells that do not normally express them (44). Microparticles deriving from apoptotic cells have been shown to carry nuclear proteins as well as nucleic acids (31,45). Filtration experiments suggested that the absence of microparticles abolished the effect of the conditioned medium to induce *PSP/reg* mRNA in naïve INS-1 cells. This suggested that cytokines, peptide hormones, or other soluble messengers present in the conditioned medium did not mediate this effect. Interestingly, heat inactivation of the conditioned medium was sufficient to inhibit *PSP/reg* mRNA expression in naïve INS-1 cells. It is therefore tempting to speculate that microparticles may contain signaling molecules or nuclear proteins which, upon uptake by neighboring cells, enhanced *PSP/reg* gene expression in these cells.

In conclusion, our study demonstrates that the execution of caspase-dependent apoptosis in INS-1 cells stimulates the induction of regenerative genes in neighboring cells, suggesting a role for MPs and PSP/*reg* in this process. These findings provide new mechanistic insights into a fundamental aspect of β-cell mass regulation.

ACKNOWLEDGMENTS

This study was supported by grants from Science Foundation Ireland (08/IN1/1949) and the Health Research Board (RP/2008/14) to J.H.M.P.; grants from the Health Research Board (RP/2007/316), the Mater Foundation cofunded by the Medical Research Charity Groups/Health Research Board, and a Mater College Grant to M.M.B; and the Swiss National Foundation (grant no. 32-66907.01) to C.B.W.

No potential conflicts of interest relevant to this article were reported.

C.B. researched data and wrote the manuscript. S.R.R., S.B., M.B., A.M.F., H.D., M.W.W., S.M.K., and C.M.B. researched data. C.G.C. reviewed/edited the manuscript and contributed to the discussion. C.B.W., R.G., and M.M.B. researched data and reviewed/edited the manuscript. J.H.M.P. wrote the manuscript and contributed to the discussion.

We thank M. Bain (Department of Cell Physiology and Metabolism, University Medical Center, Geneva, Switzerland) for excellent assistance and advice.

REFERENCES

1. Fajans SS. Scope and heterogeneous nature of MODY. Diabetes Care 1990;13:49–64
2. Yamagata K, Furuta H, Oda N, Kaisaki PJ, Menzel S, Cox NJ, Fajans SS, Signorini S, Stoffel M, Bell GI. Mutations in the hepatocyte nuclear factor-4alpha gene in maturity-onset diabetes of the young (MODY1). Nature 1996;384:458–460
3. Shih DQ, Screenan S, Munoz KN, Philipson L, Pontoglio M, Yaniv M, Polonsky KS, Stoffel M. Loss of HNF-1α function in mice leads to abnormal expression of genes involved in pancreatic islet development and metabolism. Diabetes 2001;50:2472–2480
4. Wang H, Maechler P, Hagenfeldt KA, Wollheim CB. Dominant-negative suppression of HNF-1alpha function results in defective insulin gene transcription and impaired metabolism-secretion coupling in a pancreatic beta-cell line. Embo J 1998;17:6701–6713
5. Ben-Shushan E, Marshak S, Shoshkes M, Cerasi E, Melloul D. A pancreatic beta-cell-specific enhancer in the human PDX-1 gene is regulated by hepatocyte nuclear factor 3beta (HNF-3beta), HNF-1alpha, and SPs transcription factors. J Biol Chem 2001;276:17533–17540
6. Wang H, Maechler P, Antinozzi PA, Hagenfeldt KA, Wollheim CB. Hepatocyte nuclear factor 4alpha regulates the expression of pancreatic beta-cell genes implicated in glucose metabolism and nutrient-induced insulin secretion. J Biol Chem 2000;275:35953–35959
7. Servitja JM, Pignatelli M, Maestro MA, Cardalda C, Boj SF, Lozano J, Blanco E, Lafuente A, McCarthy MI, Sumoy L, Guigo R, Ferrer J. Hnf1alpha (MODY3) controls tissue-specific transcriptional programs and exerts opposed effects on cell growth in pancreatic islets and liver. Mol Cell Biol 2009;29:2945–2959
8. Wobser H, Dussmann H, Kogel D, Wang H, Reimertz C, Wollheim CB, Byrne MM, Prehn JH. Dominant-negative suppression of HNF-1 alpha results in mitochondrial dysfunction, INS-1 cell apoptosis, and increased sensitivity to ceramide-, but not to high glucose-induced cell death. J Biol Chem 2002;277:6413–6421
9. Farrelly AM, Wobser H, Bonner C, Anguissola S, Rehm M, Concannon CG, Prehn JH, Byrne MM. Early loss of mammalian target of rapamycin complex 1 (mTORC1) signalling and reduction in cell size during dominant-negative suppression of hepatic nuclear factor 1-alpha (HNF1A) function in INS-1 insulinoma cells. Diabetologia 2009;52:136–144
10. Akpinar P, Kuwajima S, Krutzfeldt J, Stoffel M. Tmem27: a cleaved and shed plasma membrane protein that stimulates pancreatic beta cell proliferation. Cell Metab 2005;2:385–397
11. Byrne MM, Sturis J, Menzel S, Yamagata K, Fajans SS, Dronsfield MJ, Bain SC, Hattersley AT, Velho G, Froguel P, Bell GI, Polonsky KS. Altered insulin secretory responses to glucose in diabetic and nondiabetic subjects with mutations in the diabetes susceptibility gene MODY3 on chromosome 12. Diabetes 1996;45:1503–1510
12. Pontoglio M, Sreenan S, Roe M, Pugh W, Ostrega D, Doyen A, Pick AJ, Baldwin A, Velho G, Froguel P, Levisetti M, Bonner-Weir S, Bell GI, Yaniv M, Polonsky KS. Defective insulin secretion in hepatocyte nuclear factor 1alpha-deficient mice. J Clin Invest 1998;101:2215–2222
13. Hagenfeldt-Johansson KA, Herrera PL, Wang H, Gjinovci A, Ishihara H, Wollheim CB. Beta-cell-targeted expression of a dominant-negative hepatocyte nuclear factor-1 alpha induces a maturity-onset diabetes of the young (MODY)3-like phenotype in transgenic mice. Endocrinology 2001;142:5311–5320
14. Yamagata K, Nammo T, Moriwaki M, Ihara A, Iizuka K, Yang Q, Satoh T, Li M, Uenaka R, Okita K, Iwahashi H, Zhu Q, Cao Y, Imagawa A, Tochino Y, Hanafusa T, Miyagawa J, Matsuzawa Y. Overexpression of dominant-negative mutant hepatocyte nuclear factor-1α in pancreatic β-cells causes abnormal islet architecture with decreased expression of E-cadherin, reduced β-cell proliferation, and diabetes. Diabetes 2002;51:114–123
15. Wobser H, Bonner C, Nolan JJ, Byrne MM, Prehn JH. Downregulation of protein kinase B/Akt-1 mediates INS-1 insulinoma cell apoptosis induced by dominant-negative suppression of hepatocyte nuclear factor-1alpha function. Diabetologia 2006;49:519–526
16. Dor Y, Brown J, Martinez OI, Melton DA. Adult pancreatic beta-cells are formed by self-duplication rather than stem-cell differentiation. Nature 2004;429:41–46
17. Terazono K, Uchiyama Y, Ide M, Watanabe T, Yonekura H, Yamamoto H, Okamoto H. Expression of reg protein in rat regenerating islets and its co-localization with insulin in the beta cell secretory granules. Diabetologia 1990;33:250–252
18. De Caro A, Lohse J, Sarles H. Characterization of a protein isolated from pancreatic calculi of men suffering from chronic calcifying pancreatitis. Biochem Biophys Res Commun 1979;87:1176–1182
19. Terazono K, Yamamoto H, Takasawa S, Shiga K, Yonemura Y, Tochino Y, Okamoto H. A novel gene activated in regenerating islets. J Biol Chem 1988;263:2111–2114
20. Rouquier S, Verdier JM, Iovanna J, Dagorn JC, Giorgi D. Rat pancreatic stone protein messenger RNA. Abundant expression in mature exocrine cells, regulation by food content, and sequence identity with the endocrine reg transcript. J Biol Chem 1991;266:786–791
21. Watanabe T, Yonemura Y, Yonekura H, Suzuki Y, Miyashita H, Sugiyama K, Moriizumi S, Unno M, Tanaka O, Kondo H, et al. Pancreatic beta-cell replication and amelioration of surgical diabetes by Reg protein. Proc Natl Acad Sci U S A 1994;91:3589–3592
22. Graf R, Schiesser M, Lussi A, Went P, Scheele GA, Bimmler D. Coordinate regulation of secretory stress proteins (PSP/reg, PAP I, PAP II, and PAP III) in the rat exocrine pancreas during experimental acute pancreatitis. J Surg Res 2002;105:136–144
23. Garcia-Calvo M, Peterson EP, Rasper DM, Vaillancourt JP, Zamboni R, Nicholson DW, Thornberry NA. Purification and catalytic properties of human caspase family members. Cell Death Differ 1999;6:362–369
24. Canault M, Leroyer AS, Peiretti F, Leseche G, Tedgui A, Bonardo B, Alessi MC, Boulanger CM, Nalbone G. Microparticles of human atherosclerotic plaques enhance the shedding of the tumor necrosis factor-alpha converting enzyme/ADAM17 substrates, tumor necrosis factor and tumor necrosis factor receptor-1. Am J Pathol 2007;171:1713–1723
25. Leroyer AS, Isobe H, Leseche G, Castier Y, Wassef M, Mallat Z, Binder BR, Tedgui A, Boulanger CM. Cellular origins and thrombogenic activity of microparticles isolated from human atherosclerotic plaques. J Am Coll Cardiol 2007;49:772–777
26. Schiesser M, Bimmler D, Frick TW, Graf R. Conformational changes of pancreatitis-associated protein (PAP) activated by trypsin lead to insoluble protein aggregates. Pancreas 2001;22:186–192
27. Bimmler D, Angst E, Valeri F, Bain M, Scheele GA, Frick TW, Graf R. Regulation of PSP/reg in rat pancreas: immediate and steady-state adaptation to different diets. Pancreas 1999;19:255–267
28. Graf R, Schiesser M, Scheele GA, Marquardt K, Frick TW, Ammann RW, Bimmler D. A family of 16-kDa pancreatic secretory stress proteins form highly organized fibrillar structures upon tryptic activation. J Biol Chem 2001;276:21028–21038
29. Taylor RC, Cullen SP, Martin SJ. Apoptosis: controlled demolition at the cellular level. Nat Rev Mol Cell Biol 2008;9:231–241
30. Thery C, Boussac M, Veron P, Ricciardi-Castagnoli P, Raposo G, Garin J, Amigorena S. Proteomic analysis of dendritic cell-derived exosomes: a secreted subcellular compartment distinct from apoptotic vesicles. J Immunol 2001;166:7309–7318
31. Schiller M, Bekeredjian-Ding I, Heyder P, Blank N, Ho AD, Lorenz HM. Autoantigens are translocated into small apoptotic bodies during early stages of apoptosis. Cell Death Differ 2008;15:183–191
32. Zenilman ME, Chen J, Magnuson TH. Effect of reg protein on rat pancreatic ductal cells. Pancreas 1998;17:256–261
33. Butler AE, Janson J, Bonner-Weir S, Ritzel R, Rizza RA, Butler PC. β-Cell deficit and increased β-cell apoptosis in humans with type 2 diabetes. Diabetes 2003;52:102–110
34. Bonner-Weir S. β-Cell turnover: its assessment and implications. Diabetes 2001;50(Suppl. 1):S20–S24

35. Pellettieri J, Fitzgerald P, Watanabe S, Mancuso J, Green DR, Sanchez Alvarado A. Cell death and tissue remodeling in planarian regeneration. Dev Biol 338:76–85
36. Li F, Huang Q, Chen J, Peng Y, Roop DR, Bedford JS, Li CY. Apoptotic cells activate the "phoenix rising" pathway to promote wound healing and tissue regeneration. Sci Signal 3:ra13
37. Unno M, Nata K, Noguchi N, Narushima Y, Akiyama T, Ikeda T, Nakagawa K, Takasawa S, Okamoto H. Production and characterization of Reg knockout mice: reduced proliferation of pancreatic β-cells in Reg knockout mice. Diabetes 2002;51(Suppl. 3):S478–S483
38. Unno M, Yonekura H, Nakagawara K, Watanabe T, Miyashita H, Moriizumi S, Okamoto H, Itoh T, Teraoka H. Structure, chromosomal localization, and expression of mouse reg genes, reg I and reg II: a novel type of reg gene, reg II, exists in the mouse genome. J Biol Chem 1993;268:15974–15982
39. Kadowaki Y, Ishihara S, Miyaoka Y, Rumi MA, Sato H, Kazumori H, Adachi K, Takasawa S, Okamoto H, Chiba T, Kinoshita Y. Reg protein is overexpressed in gastric cancer cells, where it activates a signal transduction pathway that converges on ERK1/2 to stimulate growth. FEBS Lett 2002;530:59–64
40. Iovanna JL, Keim V, Michel R, Dagorn JC. Pancreatic gene expression is altered during acute experimental pancreatitis in the rat. Am J Physiol 1991;261:G485–G489
41. Thorel F, Nepote V, Avril I, Kohno K, Desgraz R, Chera S, Herrera PL. Conversion of adult pancreatic alpha-cells to beta-cells after extreme beta-cell loss. Nature 2010;464:1149–1154
42. Graf R, Schiesser M, Reding T, Appenzeller P, Sun LK, Fortunato F, Perren A, Bimmler D. Exocrine meets endocrine: pancreatic stone protein and regenerating protein: two sides of the same coin. J Surg Res 2006;133:113–120
43. Bianco F, Perrotta C, Novellino L, Francolini M, Riganti L, Menna E, Saglietti L, Schuchman EH, Furlan R, Clementi E, Matteoli M, Verderio C. Acid sphingomyelinase activity triggers microparticle release from glial cells. EMBO J 2009;28:1043–1054
44. Boulanger CM, Tedgui A. Dying for attention: microparticles and angiogenesis. Cardiovasc Res 2005;67:1–3
45. Orozco AF, Jorgez CJ, Horne C, Marquez-Do DA, Chapman MR, Rodgers JR, Bischoff FZ, Lewis DE. Membrane protected apoptotic trophoblast microparticles contain nucleic acids: relevance to preeclampsia. Am J Pathol 2008;173:1595–1608